A laparoscopic morcellator redesign to constrain tissue using integrated gripping teeth

Arkenbout, E. A.; den Haak, L. van; Penning, Maxime; Rog, Ellemijn; Vierwind, Amanda; van Capelle, L.E.; Jansen, F. W.; de Winter, J. C F

DOI
10.1115/1.4034882

Publication date
2017

Document Version
Final published version

Published in
Journal of Medical Devices

E. A. Arkenbout[1]
Biomechanical Engineering Department,
Faculty of Mechanical, Maritime, and
Materials Engineering,
Delft University of Technology,
Mekelweg 2,
Delft 2628 CD, The Netherlands
e-mail: e.a.arkenbout@tudelft.nl

L. van den Haak
Department of Gynecology,
Leiden University Medical Center,
Albinusdreef 2,
Leiden 2333 ZA, The Netherlands
e-mail: L.van_den_Haak@lumc.nl

M. Penning
Life Science and Technology Department,
Faculty of Applied Sciences,
Lorentzweg 1,
Delft 2628 CJ, The Netherlands
e-mail: maxime_penning@hotmail.com

E. Rog
Maritime Transport Technology Department,
Faculty of Mechanical, Maritime, and
Materials Engineering,
Delft University of Technology,
Mekelweg 2,
Delft 2628 CD, The Netherlands
e-mail: ellemijnrog@gmail.com

A. Vierwind
Life Science and Technology Department,
Faculty of Applied Sciences,
Lorentzweg 1,
Delft 2628 CJ, The Netherlands
e-mail: amandavierwind@hotmail.com

L. E. van Cappelle
Faculty of Mechanical, Maritime, and
Materials Engineering,
Delft University of Technology,
Mekelweg 2,
Delft 2628 CD, The Netherlands
e-mail: l.e.vancappelle@gmail.com

F. W. Jansen
Department of Gynecology,
Leiden University Medical Center,
Albinusdreef 2,
Leiden 2333 ZA, The Netherlands
e-mail: f.w.jansen@lumc.nl

J. C. F. de Winter
Biomechanical Engineering Department,
Faculty of Mechanical, Maritime, and
Materials Engineering,
Delft University of Technology,
Mekelweg 2,
Delft 2628 CD, The Netherlands
e-mail: J.C.F.deWinter@tudelft.nl

A Laparoscopic Morcellator Redesign to Constrain Tissue Using Integrated Gripping Teeth

Laparoscopic hysterectomy is a procedure that involves the removal of the uterus through an abdominal keyhole incision. Morcellators have been specifically designed for this task, but their use has been discouraged by the food and drug administration (FDA) since November 2014 because of risks of cancerous tissue spread. The use of laparoscopic bags to catch and contain tissue debris has been suggested, but this does not solve the root cause of tissue spread. The fundamental problem lies in the tendency of the tissue mass outside the morcellation tube to rotate along with the cutting blade, causing tissue to be spread through the abdomen. This paper presents a bio-inspired concept that constrains the tissue mass in the advent of its rotation in order to improve the overall morcellation efficacy and reduce tissue spread. A design of gripping teeth integrated into the inner diameter of the morcellation tube is proposed. Various tooth geometries were developed and evaluated through an iterative process in order to maximize the gripping forces of these teeth. The maximum gripping force was determined through the measurement of force–displacement curves during the gripping of gelatin and bovine tissue samples. The results indicate that a tooth ring with a diameter of 15 mm can provide a torque resistance of 1.9 Ncm. Finally, a full morcellation instrument concept design is provided.
[DOI: 10.1115/1.4034882]

Keywords: laparoscopic devices, minimally invasive surgery, morcellation, tissue spread, tissue constraining

[1]Corresponding author.
Manuscript received March 17, 2016; final manuscript received September 19, 2016; published online December 21, 2016. Assoc. Editor: Carl Nelson.

1 Introduction

In laparoscopic hysterectomy and myomectomy, tissue needs to be removed without compromising the integrity of the minimally invasive procedure. The power morcellator is an instrument designed for this purpose, having a fast rotating cylindrical blade that allows for the division and removal of tissue.

The food and drug administration (FDA) issued a press release in November 2014, discouraging the use of power morcellators because of their risk of spreading cancerous tissue within the abdomen and pelvis in women with unsuspected uterine sarcoma [1]. It has been estimated by the FDA that 1 in 350 women undergoing hysterectomy or myomectomy for myomas will have unsuspected uterine sarcoma [1,2]. Although this statement has been refuted and is believed to be closer to 1 in 1550 [3], these FDA statements nonetheless led to the restriction of morcellation, thereby limiting many women with symptomatic leiomyomas to total abdominal hysterectomies. Over the eight months following the FDA safety communication, a decrease of laparoscopic hysterectomies was observed together with an increase in abdominal and vaginal hysterectomies, as well as an increase in major surgical complications and hospital readmissions [3,4]. Concerns have been raised with respect to potentially higher patient morbidity and the long-term outcome of surgical techniques that are adopted as alternatives to standard power morcellation, such as the use of containment bags, vaginal incisions, and intraoperative biopsies [5]. Although complications of morcellation are rare, both the development of parasitic fibroids and the spread of sarcoma cells in the abdominal cavity have been reported [6–8]. Clearly, the issue of tissue spread caused by current power morcellators is one that requires solving.

1.1 Cause of Tissue Spread. Tissue spread is the result of a fundamental problem in morcellators that rely on the "motor peeling" mechanism [9]. The morcellation process constitutes the repetitive grasping, cutting, and disposing of tissue strips sliced from the main tissue mass. Initially, relatively long tissue strips are created. With progression of the morcellation process, that is, after the first few tissue strips have been cut and removed, the created tissue strips become shorter [10]. An explanation for this phenomenon is that the tissue mass decreases in size and weight and becomes increasingly distorted in shape. Consequently, the tissue mass itself becomes prone to being dragged along with the fast rotating cutting blade because of friction between the two. Eventually, the entire tissue mass may start rotating along with the cutting blade, thereby scattering tissue fragments throughout the intraperitoneal area.

In Fig. 1, the tissue spread problem is depicted in detail in three separate instances from left to right: (1) initiation of tissue morcellation, (2) during morcellation, and (3) morcellation failure. When initiating a morcellation action (Fig. 1, left), the tissue mass is grabbed and pulled into the morcellation tube. In the beginning, the length of the tissue strip sliced thus far (through application of force F_{pull}) is short and unable to twist significantly. Accordingly, the surgeon has proper control through force F_{pull}. However, as the slicing of the tissue strip continues, the length of the strip increases and friction between the cutting blade and the main tissue mass outside the tube can induce spinning of the mass (through force F_T), with twisting of the tissue strip as a result (Fig. 1, middle). Spinning of the main tissue mass is especially prominent when the cutting blade has dulled during its use, for example, due to having morcellated calcified myomas or unintentional

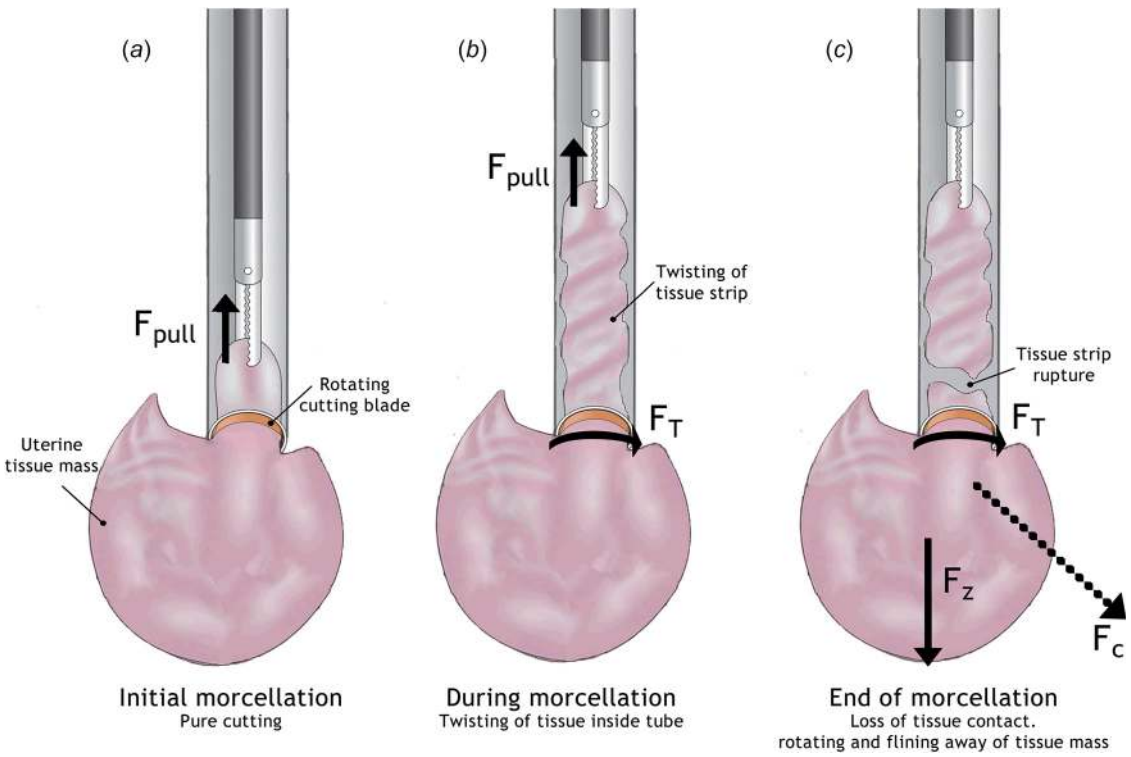

Fig. 1 Representation of the tissue mass spinning problem underlying power morcellators. (*a*) Initiation of morcellation where tissue is pulled into the morcellation tube (F_{pull}) and a tissue strip is being cut properly. (*b*) Midway through morcellating a tissue strip, where the strip has come to be of such length that twisting of the strip inside the tube occurs. This results in a (possible) torque (F_T) of the tissue mass, induced by the rotating cutting blade, spinning the tissue. (*c*) Morcellation failure due to rupturing of the (twisted) tissue strip inside the tube. The tissue mass is free to follow the torque F_T as well as disconnect from the morcellation tube (F_z), resulting in a combined force vector F_c, indicating the direction to where the tissue mass falls or is flung. Note: force vectors not to scale.

grasper–blade contact. Literature shows that a high force level is required to achieve steady-state cutting when the blade sharpness is low [11–16]. Thus, when morcellating with a dulled cutting blade, a high force F_{pull} is required to cut the tissue. A low F_{pull} will maintain tissue–blade contact but not initiate cutting, resulting in the tissue mass rotating along with the blade.

The shape of the mass, which is initially roughly spherical, is deformed due to the excision of tissue strips, increasing the likelihood of tissue scatter during tissue mass spinning. Rotation of the mass may lead to rupturing of the tissue strip (Fig. 1, right), after which the tissue mass is free to rotate with the cutting blade (F_T) and disconnect from the distal end of the morcellation tube (e.g., through gravitational force F_z). The combination of forces results in a force vector F_c, in which direction the tissue mass either falls (at low F_T) or is flung away (at high F_T).

1.2 State of the Art. In order to provide a brief overview of the state of the art with respect to morcellators, a patent search was performed in the Espacenet database using the search terms *morce* AND (instr* OR tool* OR device*),* providing 84 results. Filtering these results on title and abstract on relevance with respect to laparoscopic uterine tissue morcellation (excluding intra-uterine shavers), and removing duplicate patents from the same applicants that describe different or updated facets of the same instrument design, yielded a list of 45 relevant patents. Note that this patent search is not all inclusive as morcellator patents may exist that does not contain the string *morce**.

Standard morcellators that rely on the motor peeling working principle are abundant, where the differences between patents mostly relate to aspects such as reusability versus disposability, instrument dimensions, and cutting blade drive mechanisms [17–25]. Patents of existing morcellators include the LiNA Xcise (LiNA Medical, Glostrup, Denmark) [23], Gynecare Morcellex (Ethicon, Inc., Somerville, NJ) [17,21], and Storz Rotocut G1 (Karl Storz GmbH & Co, Tuttlingen, Germany) [26]. For a full list of current morcellators used in clinical practice, one may refer to Driessen et al. [9]. Alternative cutting mechanisms include oscillating or vibrating cutting blades [27,28], electrosurgical cutting [29–36], waterjet cutting [37], grinding [38], or the use of a wire mesh to slice tissue [39–41]. Each of these alternative cutting methods has its own strengths and weaknesses. An instrument having an oscillating cutting blade is the MOREsolution Tissue Morcellator (AxtroCare/BlueEndo, Lenexa, KS), which alternately turns four times clockwise and four times counterclockwise. Although this instrument has shown to provide less tissue spread when in oscillation mode as compared to rotation mode [42], the oscillating mode still uses full blade rotations. Electrosurgical cutting speed is dependent on power settings [43], and smoke may obscure the surgeon's vision [44] and contain carcinogenic agents [45]. Using waterjet cutting as a morcellation method macerates the tissue, potentially creating tissue spill in the process, and making histological evaluation no longer possible [46]. Finally, wire mesh cutting is a method that encapsulates the tissue mass and subdivides it into multiple smaller pieces by drawing the wire mesh through the tissue [39–41]. This method may be time-consuming, as the time required to manipulate a tissue mass into the encapsulating bag has been reported to range from 1 to 13 min [47,48].

To catch and contain tissue spread, a number of laparoscopic tissue entrapment bags have been proposed, each with their own material properties with respect to robustness against perforations and number of openings [49–58]. Following the FDA safety communication, several studies have been performed to evaluate the safety and applicability of such bags in combination with current morcellators [47,59–61]. Alternatively, several patents describe the bag as inherent parts of the morcellation mechanism [29,32,62–65].

Finally, the transport of tissue through the morcellation tube can either be done manually, as is current standard practice using a laparoscopic grasper, or automatically, either through suction [29,32,64,66], an internal auger [38], or screw thread [67]. The method of tissue transport strongly relates to the way the surgeon is able to control the uterine tissue mass. The standard morcellator with a laparoscopic grasper may cause tissue scatter problems as described above, whereas automated transport mechanisms usually have some additional way of constraining the tissue. Three patents specifically describe mechanisms that provide improved tissue control [68–70]. The first patent describes an additional instrument that constrains the tissue mass and allows it to be presented to the morcellator in the best way possible [68] (Fig. 2(*a*)). The remaining patents describe a morcellator with grasping jaws at their distal end to confine the tissue at the time of cutting (Figs 2(*b*) and 2(*c*)). The use of such components is beneficial to close the force loop near the cutting mechanism.

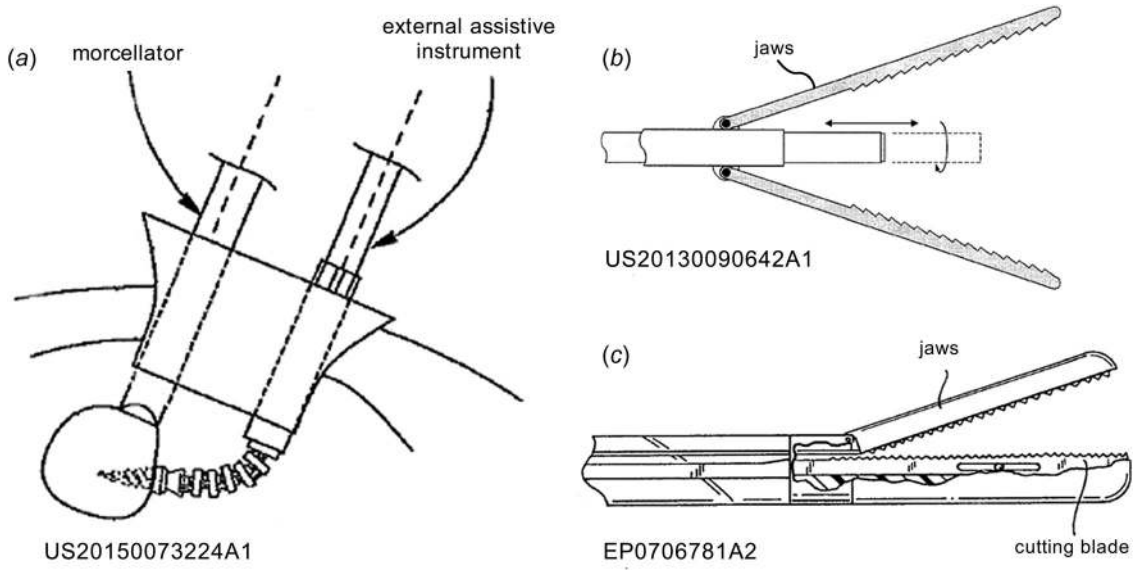

Fig. 2 Patent morcellator designs that engage and constrain the main tissue mass during morcellation. (*a*) Patent US20150073224A1 [68], (*b*) patent US20130090642A1 [70], and (*c*) EP0706781A2 [54]. Images cropped and component numbers removed from original patents.

1.3 Proposed Solution. Solutions identified in the literature to solve the issue of tissue spread are to introduce an alternative cutting method, to encapsulate the specimen being morcellated, or to enhance the efficacy of the rotational cutting mechanism itself. The use of an alternative cutting method has already been explored extensively, but the rotating cutting blade method has remained the standard. The use of a bag is feasible but does not address the source of the problem that causes tissue spread. Furthermore, studies have shown that up to 30% of bags used to contain morcellation spillage may exhibit leakage [71–73], and contained morcellation may not prevent metastasis of high-grade tumors, despite having used a bag [74,75]. The current research focuses on enhancing the efficacy of the current motor peeling principle to reduce tissue scatter, an approach that may be complementary to the use of bags. Our approach locally confines the tissue mass during morcellation, such as shown in the patents presented in Figs. 2(*b*) and 2(*c*), thereby preventing the tissue mass from spinning with the rotating blade. Our design differs from those shown in Fig. 2 in that the method of tissue confinement is integrated in the standard morcellation instrument, rather than using an external fixation method such as the jaws shown in Figs. 2(*b*) and 2(*c*). Moreover, our design does not require a change in the standard tissue cutting method.

2 Concept Design

Many animals can be found that make clever use of tooth geometries and configurations. For example, a method seen in nature for holding and swallowing (slippery or struggling) prey, are large and backward facing pointed papillae. These cover the tongue and roof of the mouth of the penguin for eating arrow squids [76], and the upper and lower jaws of the leatherback sea turtle, to aid in the consumption of jellyfish [77,78]. Examples of animals that prey on fish or mammals larger than themselves are the cookie cutter shark (Isistius brasiliensis) and the lamprey (Petromyzontiformes, Fig. 3(*a*)), which both behave much like a morcellator. Using a mouth and saw teeth that are adapted for sucking, the small shark maintains an attachment to its prey, and is able to slice and scoop out chunks of tissue by using its lower band of saw teeth while rotating its entire body [79,80]. Similarly, using suction and a vast array of teeth arranged in whorls around the mouth opening, the lamprey attaches itself to other fish. The tongue, also having teeth, is subsequently used to rasp away flesh from the host.

Taking cues from nature, a viable solution to improving the efficacy of morcellators may be through the integration of teeth to provide grip on the tissue mass. In specific, these teeth should compensate for forces F_T and F_Z. An example of a morcellator design we have created with this principle in mind is provided in Fig. 3(*b*), where teeth have been integrated into the instrument tip. In order to investigate the potential of this solution, a proof-of-principle design has been made of a single ring of teeth. These teeth are required to generate a reaction force close to the location where force F_T is generated by the blade, thereby locally closing the force loop in the event of spinning of the tissue mass. The teeth should engage the tissue mass only when it starts to rotate with the blade, and not hinder the normal tissue debulking process of the morcellator.

The design of the ring of teeth (Fig. 3(*c*)) is such that it can be placed coaxially on the inside of the circular rotating blade, at the distal end of a standard morcellation tube. The geometry and orientation of the teeth ensure that they hook into the tissue mass when it starts to rotate with the blade. The teeth are angled inward, into the morcellation tube, freely allowing the tissue to be pulled up the tube, but blocking it from sliding back into the peritoneal area.

This paper presents research into the dimensions and number of teeth to achieve an optimal gripping force on the tissue mass, while still allowing the pulling of the debulked tissue strip through the morcellation tube. Test-bench trials have moreover been performed to assess the grip strength of the teeth on animal muscle tissue.

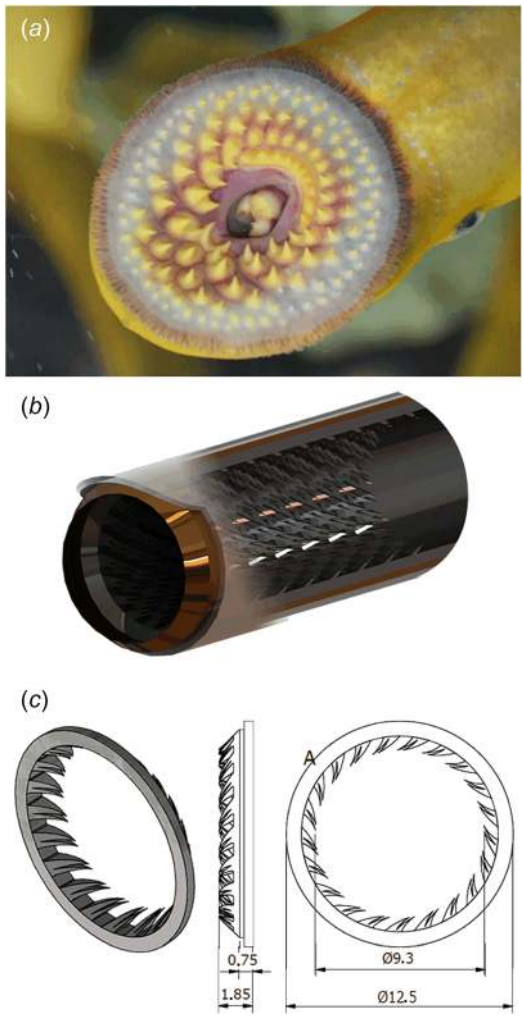

Fig. 3 (*a*) Lamprey. Image edited to only show the mouth [93], (*b*) lamprey inspired morcellation instrument tip, having integrated teeth for tissue traction, and (*c*) design of a single teeth ring. Dimensions are in millimeters.

3 Method

The measurements and validation of the proposed design were performed in two stages together comprising six measurement sessions. First, through porcine gelatin tests (measurement sessions 1–4), teeth of various dimensions were assessed in order to motivate the design choices made in prototyping a single teeth ring. The second stage of tests (measurement sessions 5 and 6) provided the quantification of this ring in terms of gripping strength when using bovine muscle tissue. For all measurements, a force–displacement curve was obtained by drawing a sample of gelatin or animal tissue past the teeth. The sequence in which the six measurements sessions were performed is shown in Fig. 4. The selection process of tooth geometries based on measured forces is described in the subsequent Methods sections (see also Fig. 4, "selection" boxes); the actual force values are provided in the Results section.

3.1 Teeth Optimization for Tissue Grip—Gelatin Tests. To study the tooth geometry and measure their maximum gripping force, a test setup was created as shown in Fig. 5. A 1.0 mm thick metal plate, containing sets of teeth, could be placed under an

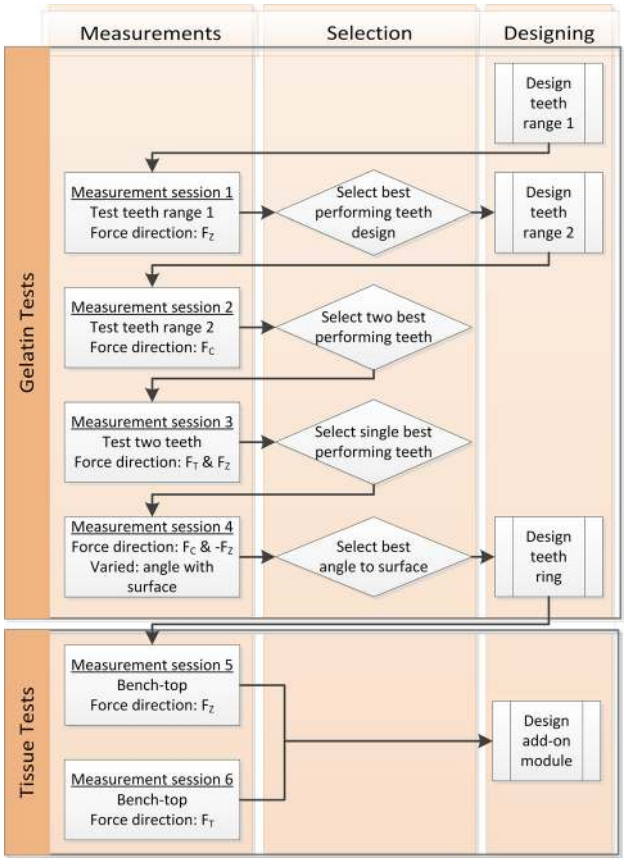

Fig. 4 Flowchart of the sequence of measurements performed, where at each measurement a force–displacement curve was generated. In measurement sessions 1–4, porcine gelatin samples were pulled over the indicated teeth in the directions F_T, F_C, or F_Z (Fig. 1), using the test setup shown in Fig. 5. In measurement sessions 5 and 6, animal tissue samples were pulled in directions F_Z and F_T, in contact with the teeth ring, using the test setup shown in Fig. 8.

angle of 30 deg, 45 deg, or 60 deg with respect to the smooth horizontal surface (see annotation in Fig. 5(*b*)) so that only the teeth were protruding upward. A spring-loaded mechanism under the metal plate was used to center the plate parallel and flush with respect to the surface. Two metal plates of various sets of teeth were created (Fig. 6). The three angles with respect to the horizontal surface were chosen to span a range that is likely to show an influence on the measured forces. Only three angles were assessed to keep the number of measurements to a manageable size. Assessing the fine-grained influence of the gripping angle is left for future research.

Measurements involved placing a set of teeth in the middle of the surface and a gelatin sample in front of them. The gelatin sample consisted of 15% gelatin and 85% water. A pulling wire (fishing thread, 0.2 mm diameter) ran from a load cell (Futek LSB200, 10 lb), having a force measurement range of 0–45 N and resolution of 0.038 N, to the gelatin block and back. The wire was placed around the sample with a small plate at the back, allowing the pulling force to be distributed equally over the back surface of the sample. The load cell was attached to a linear stage having a movement step size of 1 μm and speed of 1.25 mm/s. By generating a force–displacement curve while drawing samples past the teeth, the peak gripping force (i.e., the highest measured force, F_{max}) could be measured in different pulling directions (F_Z, F_T and F_C, Fig. 5). For each sample, the front-facing surface contacting the teeth had dimensions 24 × 17 mm. A roof plate was placed closely above, but initially not contacting, the gelatin samples (not shown in Fig. 5), vertically constraining them from (upward) escaping the grasp of the teeth. The friction forces resulting from contact between the sample and both the horizontal surface and the roof plate were measured separately and subtracted from the results. Not all teeth were measured in all force directions and under all combinations of conditions in order to keep the amount of measurements to a manageable number. A total of 194 measurements were performed in measurement sessions 1 through 4, with each measurement taking about 4 min.

3.1.1 Measurement Session (1): Gripping Force at Teeth of Different Geometry. With the goal of finding a well-performing tooth geometry, various teeth were assessed (Fig. 6, top). These teeth had a constant height of 1.0 mm, and were varied in wedge angle (range 20 deg and 60 deg, see teeth A, B, C, and I), curvature (linear or radius of 1.0 or 2.0 mm, see teeth E, F, and H), combinations of teeth (D and F), and blunt teeth (G). For this measurement session, the teeth were kept under a 45 deg angle with respect to the horizontal surface (Fig. 5(*b*)). This angle was the midrange value around which a high gripping force was expected to be measured. Force direction F_Z was assessed. The total number of measurements performed was 54 (nine different tooth geometries * six measurements per geometry).

3.1.2 Measurement Session (2): Gripping Force at Teeth of Different Width and Height. The results of measurement session 1 showed that tooth geometry D (Fig. 6, top), having a combination of two differently sized teeth, generated the highest maximum gripping force (for full results, see Sec. 4.1). These teeth were redesigned to function in force direction F_T by curving them in a 45 deg angle sideways (Fig. 6, bottom), and were varied in height

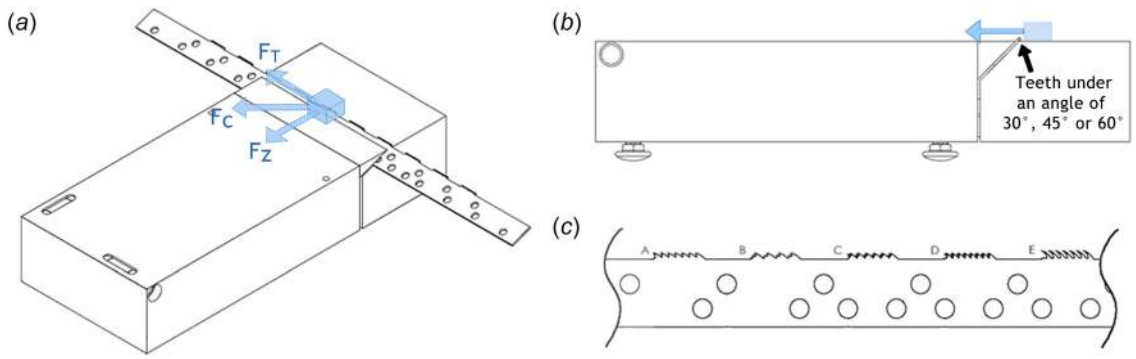

Fig. 5 (*a*) Three-dimensional view of the gelatin and teeth test setup, (*b*) side view of the setup, and (*c*) example of the teeth that have been evaluated. A gelatin sample (small block) was placed near the teeth, which were placed under an angle. Pulling the sample in the force directions F_Z, F_T, and F_C, (as also shown in Fig. 1) evaluated the gripping force the teeth had on the sample in that specific direction. Force–displacement measurements were performed with a tensile tester.

(1.0, 1.5, and 2.0 mm). The teeth also varied in width by equally distributing their number (range 4–8) over a length of 10 mm. Both "combined teeth" (e.g., Fig. 6, bottom, tooth geometry B) and "singular teeth" (e.g., Fig. 6, bottom, tooth geometry A) were designed. Measurements were performed in force direction F_C, while again keeping the teeth under a 45 deg angle with respect to the horizontal surface. Total number of measurements performed was 80 (ten types of tooth geometries * eight measurements per geometry). Figure 6 (bottom) provides an overview of the ten teeth that were tested in measurement session 2.

3.1.3 Measurement Session (3): Gripping Force in All Force Directions. From measurement session 2, teeth F and J (Fig. 6, bottom) were found to have the highest mean maximum gripping force (F_{max}) in force direction F_C (for full results, see Sec. 4.1). These teeth were further assessed in force directions F_T and F_Z, while still keeping their angle with respect to the horizontal surface at 45 deg. Total number of measurement performed was 24 (two types of tooth geometries * six measurements per geometry * two force directions).

3.1.4 Measurement Session (4): Gripping Force for Different Teeth Angles With Respect to the Horizontal Surface. Following measurement session 3, tooth geometry J (Fig. 6, bottom) was found to provide the highest gripping force (F_{max}). Having already quantified the teeth in all force directions at a 45 deg angle with respect to the horizontal surface (Fig. 5(*b*)), this angle was varied to 30 deg, 45 deg, and 60 deg. The maximum gripping force was measured in force directions F_C and the inverse direction of F_Z (i.e., $-F_Z$). $-F_Z$ was used to quantify the force required to draw a gelatin sample over the teeth in their nongripping direction, which

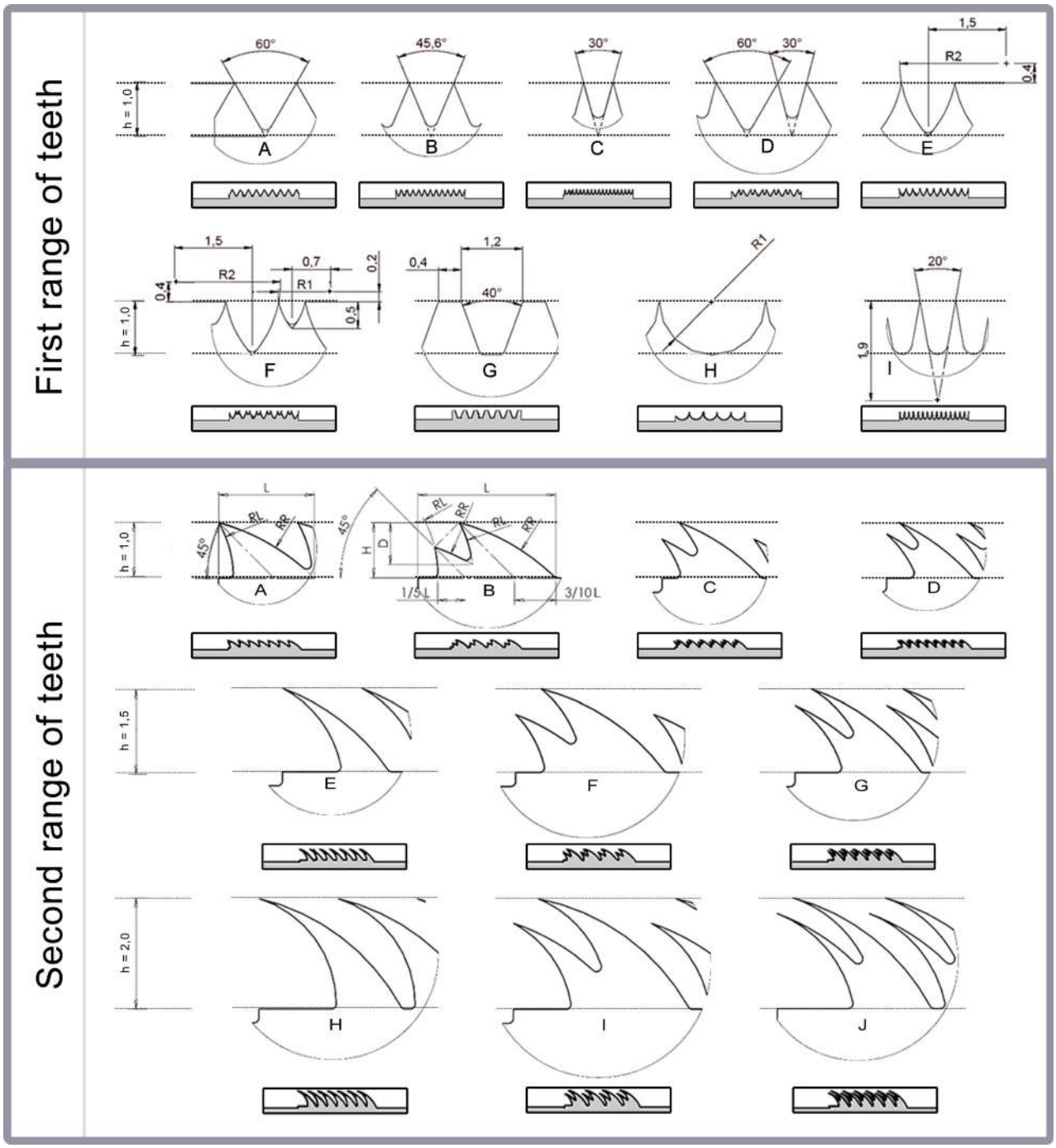

Fig. 6 First (top) and second (bottom) range of teeth evaluated in measurement session 1 and sessions 2–4, respectively

Fig. 7 Prototyped steel teeth ring, using tooth geometry *J* (Fig. 10, bottom), 2.0 mm height, 1.4 mm width, 0.3 mm spacing between teeth, and 45 deg inward angle. The ring has 21 teeth.

is equivalent to drawing tissue into the morcellator tube in a clinical scenario. Total number of measurement performed was 36 (six measurements * two force directions * three angles with respect to the horizontal surface).

3.2 Teeth Ring Assessment for Tissue Grip—Bovine Tissue Tests. Through the design-oriented measurement sessions 1–4, tooth geometry J (teeth of 2.0 mm height and 1.4 mm width, 0.3 mm spacing between teeth, and a 45 deg angle with respect to the horizontal surface) was selected to be developed into a teeth ring (Fig. 7). This teeth ring was assessed in measurement sessions 5 and 6, in force directions F_T and F_Z, respectively, using the test setup shown in Fig. 8 and the same linear stage as used in sessions 1–4. Here, the teeth ring was attached to the end of a tube with outer diameter 12.5 mm and inner diameter 11.0 mm, which is approximately equal to the size of most current morcellation instruments. Bovine muscle tissue strips were collected from three larger tissue samples. The strips, each with size $10 \times 10 \times 40$ mm, were cut in four different directions, assuring an equal distribution of muscle striations among all tissue samples. Each sample was clamped in the test setup by pulling it for a set distance into the fixation tube and placing a pin all the way through the tissue sample. The tissue strip was drawn into the morcellation tube and a 5 mm distance was kept between the fixation and morcellation tube.

3.2.1 Measurement Session (5): Gripping Force at Tissue Translation. Tissue placed inside the morcellation tube was pulled out of the tube by translating the fixation tube backward over a distance of 12 mm. First, nine measurements (i.e., three tissue strips, each used three times) were used to measure the friction resistance of the morcellation tube in the absence of gripping teeth. Next, 45 measurements (15 tissue strips, each used three times) were performed, measuring the maximum gripping force (F_{max}) of the ring of teeth.

3.2.2 Measurement Session (6): Gripping Force at Tissue Rotation. Finally, tissue placed inside the morcellation tube was rotated by rotating the fixation tube by approximately 2.7 turns (by translating the linear stage over a distance of 107 mm). As in measurement session 5, first nine measurements were performed without involving the gripping teeth to ascertain the friction resistance of the morcellation tube itself. Next, 60 measurements were performed, divided over 15 tissue strips, where each strip was measured four times. At each strip, the first three measurements involved rotating the tissue *against* the pointing direction of the teeth. During the fourth measurement, the tissue was rotated *along with* the pointing direction of the teeth, to measure the force required to rotate tissue free from the gripping teeth.

Differences between the tooth geometries were assessed using a one-way analysis of variance (ANOVA) with the Tukey–Kramer method and a significance level α of 0.05.

4 Results

4.1 Teeth Optimization for Tissue Grip—Gelatin Tests. An example of a force–displacement curve of a measurement where a block of gelatin was drawn into teeth D of teeth range one is shown in Fig. 9(*a*). At a displacement of 0 mm, the gelatin sample was right up against the teeth but not yet drawn into them. At continued displacement, the teeth dug into the sample and elastic deformation of the sample occurred while the measured force

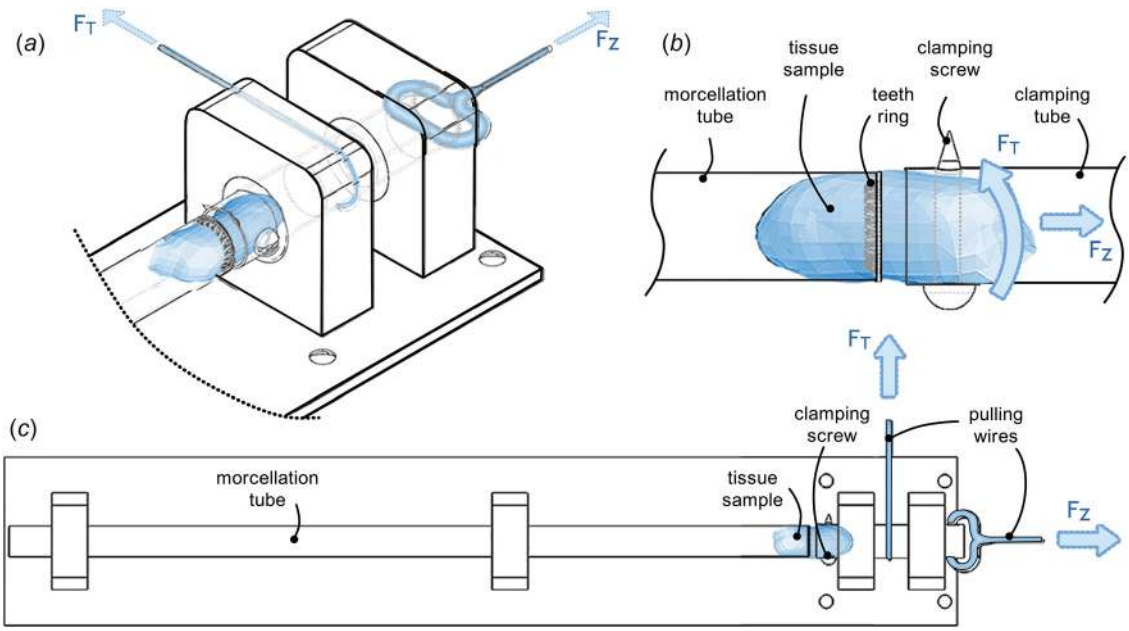

Fig. 8 (*a*) Three-dimensional view of the bovine tissue and teeth test setup, (*b*) close-up of tissue sample clamped and subjected to forces F_Z or F_T while in contact with the teeth ring, and (*c*) top view of the setup. A tissue sample is placed in contact with the teeth, which is mounted at the end of the morcellation tube. Pulling or rotating the sample in the force directions F_Z or F_T, as also shown in Fig. 1, evaluates the grip the teeth have on the sample in that specific direction. Force–displacement measurements were performed with a tensile tester.

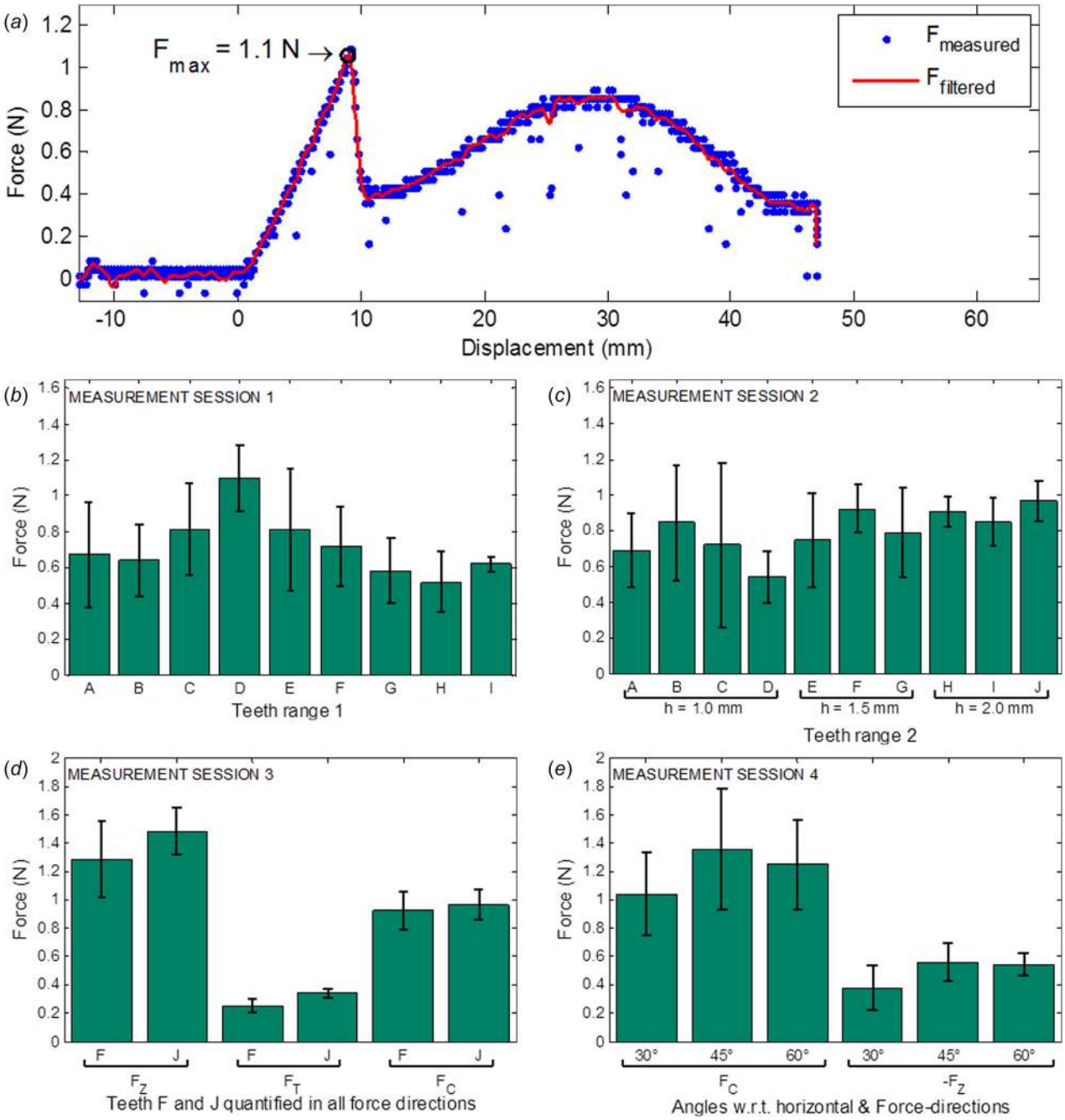

Fig. 9 (*a*) Characteristic sample measurement (teeth range 1, teeth type D, measurement session 1). The maximum grip force on the gelatin sample is indicated by F_{max}. (*b–e*) Results of measurement sessions 1 through 4. All results are presented as mean ± SD gripping force. (*b*) Measurement session 1: force generated by various tooth geometries in force direction F_Z. (*c*) Measurement session 2: force generated by various geometry and size teeth in force direction F_C. (*d*) Measurement session 3: force generated by teeth types *F* and *J* in force directions F_Z, F_T and F_C. (*e*) Measurement session 4: force generated by tooth geometry *J* in force directions F_C and inverse of F_Z (i.e., $-F_Z$), each for three different angles of the teeth with respect to the horizontal surface.

sharply rose. At the force peak (F_{max}), the sample material started to rupture. As a result, the teeth lost grip and the measured force dropped sharply. At continued displacement, the sample was drawn over and through the teeth, where the second rise and drop in grip force can be attributed to the teeth regaining their grip on the gelatin sample.

4.1.1 Measurement Session (1): Gripping Force at Teeth of Different Geometry. Means and standard deviations of F_{max} at all teeth of the first teeth range (Fig. 6, top), measured in force direction F_Z, are presented in Fig. 9(*b*). The ANOVA revealed a significant difference between tooth geometries, ($F(8,45) = 3.56$, $p = 0.003$). Teeth type D provided the highest mean F_{max}. This difference is statistically significant compared to teeth types A, B, G, H, and I ($p_{A\text{-}D} = 0.043$, $p_{B\text{-}D} = 0.022$, $p_{G\text{-}D} = 0.007$, $p_{H\text{-}D} = 0.001$, $p_{I\text{-}D} = 0.015$). A possible explanation why teeth type D outperforms the other teeth types may be that it uses a combination of two different teeth types (A and C). The depth of the teeth alternate among each other, which may have an effect on the location from where the gelatin sample starts to rupture.

4.1.2 Measurement Session (2): Gripping Force at Teeth of Different Width and Height. Means and standard deviations of F_{max} for all teeth of the second teeth range (Fig. 6, bottom),

measured in force direction F_C, are presented in Fig. 9(*c*). According to the ANOVA, the tooth geometries were significantly different from each other ($F(9,70) = 2.30$, $p = 0.025$). The two teeth types with the highest mean F_{max} were *F* and *J*, with 0.92 N (SD = 0.13 N) and 0.97 N (SD = 0.11 N), respectively. Only teeth *J* was statistically significantly different from teeth D ($p_{D\text{-}J} = 0.021$).

As the teeth height was varied between $h = 1.0$ mm, 1.5 mm, and 2.0 mm, grouping those respective gripping forces together gave 0.70 N (SD = 0.31 N), 0.82 (SD = 0.23 N), and 0.91 N (SD = 0.12 N), respectively. According to the ANOVA, these three means were significantly different from each other, $F((2,77) = 5.19$, $p = 0.008$). The mean force for teeth with a height of 2.0 mm was statistically significantly higher compared to the mean force of teeth 1.0 mm in height ($p = 0.006$). No statistically significant difference was found for the teeth having a height of 1.5 mm as compared to the other teeth. The teeth providing the highest mean gripping force of both the 1.5 mm and 2.0 mm teeth height groups, being teeth *F* and *J*, were selected to be further investigated.

4.1.3 Measurement Session (3): Gripping Force in all Force Directions. Measuring the gripping force of teeth types *F* and *J* in all force directions yielded the results as shown in Fig. 9(*d*). Teeth type *J* outperformed *F* in all measurements, although this difference is only statistically significant in direction F_T ($F(1,10) = 13.33$, $p = 0.004$).

4.1.4 Measurement Session (4): Gripping Force for Different Teeth Angles With Respect to the Horizontal Surface. Measuring teeth type *J* (Fig. 6, bottom) while varying their angle with respect to the horizontal surface (Fig. 5(*b*)) resulted in Fig. 9(*e*). Force directions F_C and the reverse of F_Z (i.e., $-F_Z$) had been assessed. In the direction of $-F_Z$, the force should have been as low as possible, as this represents the resistance of the sample when drawing it along with the facing direction of the teeth, rather than opposing them. No statistically significant differences were observed. For the design of the teeth ring, the aim was to generate a gripping force in the direction of F_C as high as possible. Accordingly, the choice for teeth type *J* under an angle of 45 deg was made.

4.2 Teeth Ring Assessment for Tissue Grip—Bovine Tissue Tests

4.2.1 Measurement Sessions (5) and (6): Gripping Force at Tissue Translation and Rotation. Measurements were performed using bovine tissue, assessing the gripping force in force directions F_Z and F_T, by, respectively, translating and rotating tissue while in contact with the teeth ring. The teeth ring was designed using teeth type *J* (see Fig. 6) under an inward angulation of 45 deg with respect to the morcellation tube. All tissue strips had been measured three times. Separating the measurements into groups based on their trial number yielded the results shown in Fig. 10(*a*). No significant differences were observed in the F_Z force direction. However, the ANOVA showed a significant difference between trials in the F_T force direction ($F(2,42) = 8.01$, $p = 0.001$) (see Fig. 10(*b*)). The gripping force for the first trial was significantly higher compared to subsequent trials ($p_{\text{trial 1 –trial 2}} = 0.019$, $p_{\text{trial 1 – trial 3}} = 0.001$), potentially a result of tissue damage caused by the teeth. In the force direction F_Z, all the data were therefore grouped. However, in the direction F_T, the first time a tissue strip was measured was considered separately from subsequent trials.

The results for both force directions, measured both against and along with the teeth, are shown in Fig. 10(*b*).

4.3 Instrument Design. The tests performed in measurement sessions 5 and 6 with the teeth ring yielded a maximum gripping force of 1.67 N (SD = 0.93 N) in the F_Z direction, and 2.32 N (SD = 1.00 N) and 1.44 N (SD = 0.53 N) in the F_T direction for the first and subsequent trials, respectively. Because existing

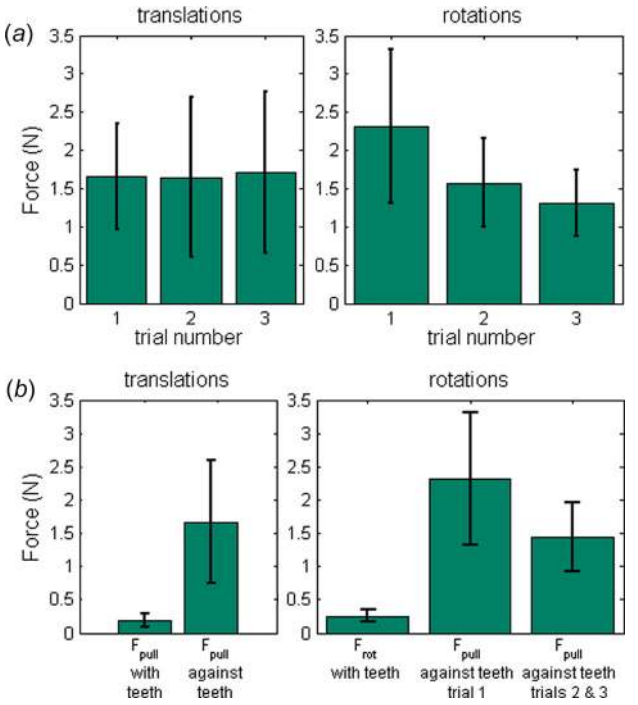

Fig. 10 Results of measurement sessions 5 and 6. (*a*) Mean ± SD maximum teeth gripping force in force directions *Fz* and *Fc* (translations and rotations plot, respectively). Three measurement trials were performed per tissue strip, and results are group per trial number. (*b*) Results of measurement sessions 5 and 6. Mean ± SD of the maximum teeth gripping force pulled along with and against the pointing direction of the teeth, respectively.

morcellators vary in diameter, it is interesting to extrapolate these results [9]. Considering that the teeth ring had 21 teeth that were equally distributed along its inner diameter ($\varnothing_{inner} = 11.5$ mm), a teeth ring integrated into a morcellator with an outer diameter of 15 mm and wall thickness 0.5 mm (leading to $\varnothing_{inner} = 14$ mm) would have 25 teeth. Such a teeth ring would provide 2.76 N of gripping force in the F_T force direction the first time that grip is generated (assuming that all teeth grip the tissue equally). Assuming that the gripping force is a linear function of the number of teeth, scaling up the diameter of the morcellation tube to 20 and 30 mm (thereby matching for example the 20 mm diameter of the Morce Power Plus (Richard Wolf, Germany) [81] and the 30 mm diameter of a proposed transvaginal morcellation design [82]) would provide 3.76 N and 5.74 N of grip force, respectively. The function that relates torque to radius ($\tau = r \cdot F$) shows that for a tube of 15 mm diameter, a single teeth ring can counteract a torque up to 1.93 Ncm (= 0.7 cm * 2.76 N). For diameters of 20 and 30 mm, this would be 3.57 Ncm and 8.32 Ncm per teeth ring, respectively.

Torques of cutting blades reported in literature range from 80 N cm (TCM3000BL Morcellator, Nouvag [83]) to 1.5 Nm (MoreSolution, Axtrocare [84]), whereas the RPM of morcellators ranges from 50 to 2000 RPM (TCM3000BL Morcellator: 50–1000, MorseSolution: 100–800). Torque is inversely related to RPM, and thus morcellators that allow for higher RPM have a lower maximum torque. The optimal torque–RPM setting likely depends on the tissue type, the diameter of the morcellation tube, and the pulling force (F_{pull}) with which the tissue is presented to the blade. Extrapolating the measured torque resistance for a single teeth ring to a series of stacked rings yields an estimated torque resistance of 38 Ncm, assuming 20 stacked rings over a length of 30 mm and a tube diameter of 15 mm (Fig. 3(*b*)). This torque resistance accounts for approximately half of the possible maximum torque generated by for example for the TCM3000BL

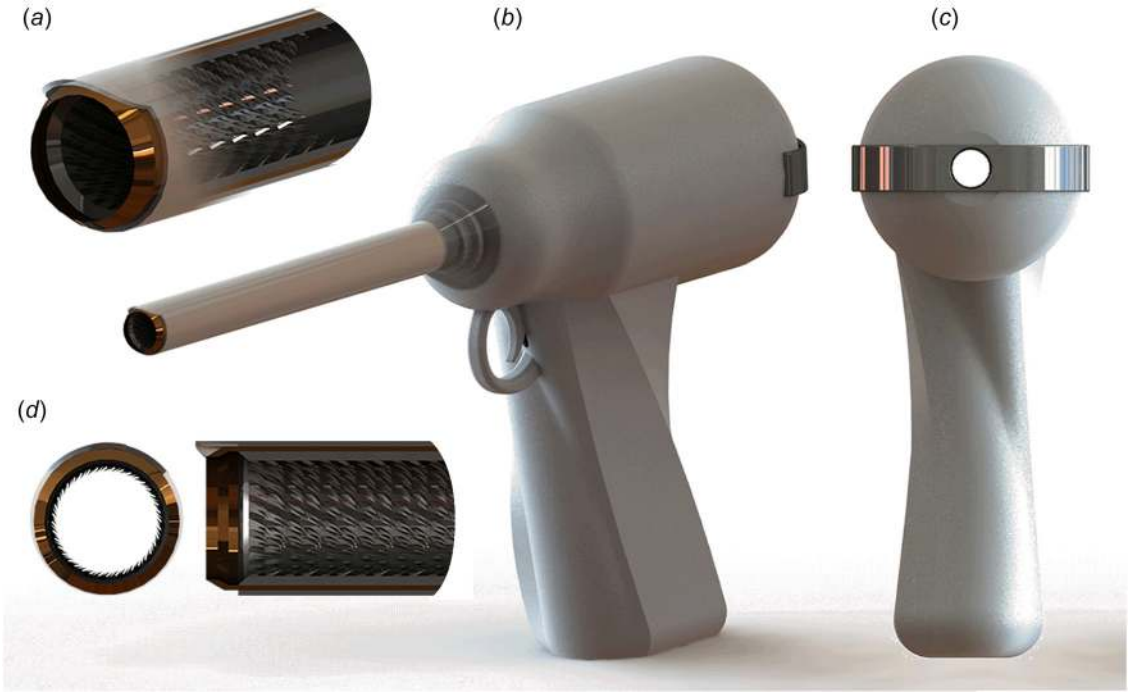

Fig. 11 Concept design of a generic morcellator combined with an add-on module providing a passive inner morcellation tube with teeth rings that hook into the tissue strip at the occurrence of tissue mass spinning. (*a*) The add-on module connects to the morcellator through a clamping mechanism at the back-end. (*a*) Three-dimensional zoom-in on instrument tip, (*b*) full 3D model, (*c*) back view of model and (*d*) front view and side view with cross section of instrument tip.

Morcellator [83]. The gripping force generated by 20 stacked rings in the direction along with the teeth is estimated to be 4.7 N (0.2 N * (25 teeth/21 teeth) * 20 rings); hence, the required pulling force (F_{pull}) to be supplied by the surgeon to the tissue mass only increases slightly. Although this is an approximate calculation, it does show that it is theoretically possible to use teeth to compensate for force $F_{T.}$ A full concept design of a morcellator is provided in Fig. 11. Future research should be conducted to experimentally validate the estimated torque resistances, and to integrate the stacked rings into an existing morcellation instrument.

5 Discussion

This paper presented the iterative design and evaluation of gripping teeth for the purpose of constraining tissue mass in the advent of its rotation along with the morcellation cutting blade. The measurements suggest that a series of stacked teeth rings can provide an adequate torque resistance for this purpose. Several measurement and design limitation have to be considered, however.

5.1 Measurement Limitations. Measurement sessions 1 through 4 used porcine gelatin samples to evaluate the gripping strength of teeth of varying geometry, and empirically determine which geometry performed the best. The use of gelatin was advantageous as it allowed for a large number of measurements within a short time frame, was readily available, and had an elasticity modulus comparable to that of actual tissue. Gelatin is frequently used for needle–tissue interaction investigations and its force–position curve is linear. In contrast, bovine tissue is nonlinear and has a rupture toughness that differs from gelatin [85]. Therefore, the results from measurement sessions 1 through 4 have to be assessed relative to each other and should not be compared with sessions 5 and 6 in absolute terms.

Bovine muscle tissue is striated by nature, whereas the female uterus consists of smooth muscle tissue. Human uterine tissue or smooth muscle tissue that resembles the human uterus is not readily available for testing. For this reason, measured gripping force levels may be different from a true clinical scenario. In our research, the tissue strips were cut in various directions to obtain a roughly equal distribution in striation directions, thereby compensating for the influence of striations. An additional limitation of the measurements was that the tissue strips were precut. Therefore, the shape of morcellated tissue strips created during clinical procedures was not a factor that influenced our results. Finally, the measurement results represent a quasi-static scenario because the tissue was slowly drawn through the teeth. The speed of tissue translation or rotation was not varied.

Not all observed differences in teeth gripping forces were statistically significant at each individual measurement session. However, through the successive design process (Fig. 4), this research iterated toward a single teeth design. This process was an efficient alternative to testing all teeth across all possible variations, angles, and force directions. The current design, however, may represent a local optimum in the design solution space, and further refinements may be possible.

5.2 Teeth Design. The measurement results in this research were used to come to a teeth design that provided the largest gripping force in specific force directions. These teeth were subsequently integrated into a proof-of-principle design for future validation and quantification.

The measurements were not intended to provide a deep understanding of the relation between tooth parameters (e.g., geometry and sharpness), tissue properties (e.g., elasticity and viscosity), or crack formation. Although the ability to grasp tissues (e.g., the gall bladder or colon) with laparoscopic graspers without causing tissue damage is important for clinical practice [86], the amount of published research into the design of gripping teeth with respect to pinching force, tissue damage, and tissue slippage is limited [86–91]. One factor of importance is the curvature of individual teeth, where an increase of radius results in reduced tissue

damage at the expense of gripping strength [87–90]. During morcellation, the degree of tissue damage is not important; hence, in this research, only aggressive teeth were assessed. In the literature, both 1.0 mm and 2.0 mm sized teeth have been tested, resulting in no clear differences in gripping forces between these two designs [88,89]. This is in agreement with the present results (Fig. 9(*c*)). However, the results in the literature have been obtained for straight symmetrical teeth, comparable to the teeth tested in measurement session 1 (Fig. 6, top). To the best of our knowledge, no results are available in the literature with respect to angled teeth such as those used in measurement sessions 2, 3, and 4 (Fig. 6, bottom).

An interesting finding was that the best-performing tooth geometry consisted of two different sized teeth (teeth D, Fig. 6, top). Compared to a single teeth design (e.g., teeth A, Fig. 6, top), there may be a difference in crack formation and propagation because the depths with which the tissue can sink in between the teeth alternate between 0.85 mm and 0.65 mm. However, teeth *F* (Fig. 6, top) also consisted of two differently sized teeth, yet did not exhibit the same performance as teeth D. The underlying mechanism behind the effects of alternating teeth requires further investigation.

The design of the teeth is a trade-off between gripping forces in the F_T and F_Z force directions and the obstruction force $-F_Z$. These forces are a function of teeth size, tooth geometry, number of teeth, and their angle with respect to the horizontal surface. When stacking multiple teeth rings in a row, the relative spacing between the rings will be another factor that determines the amount of tissue grip generated. One can make a comparison in this regards to fenestrations (i.e., openings) in laparoscopic graspers, where it has been theorized that fenestrations allow the tissue to bulge into them, thereby achieving a form-fit between tissue and grasper. Literature provides contradicting evidence regarding the effects of fenestrations for creating tissue grip [89,91], thus providing no indication regarding the distance that teeth need be apart.

Finally, the structural integrity of the tissue strip is of importance for the level of gripping force that can be obtained with the teeth. This is evidenced by the difference that was observed in the F_T force direction between the first and subsequent trials. This finding suggests that the initial gripping force generated on tissue mass at the onset of tissue mass rotation should directly be of adequate level to prevent the mass from spinning.

5.3 Instrument Design and Optimization. In essence, by using teeth to prevent the tissue mass from spinning, one is removing the surgeon from the "force loop" near the cutting blade. In the standard morcellator design, the influence of the surgeon is limited to applying a pulling force F_{pull}, whereas in order to prevent the tissue mass from spinning, the surgeon should also be able to rotationally constrain the tissue mass. It is possible, but impractical, to leave this to an assisting surgeon who makes use of a laparoscopic grasper disposed through a different trocar. By integrating gripping teeth designed to compensate for force F_T while not hindering tissue strip cutting and transport, the tissue mass is controlled without actually having to change the standard morcellation process. Moreover, by preventing the tissue mass from spinning, the amount of tissue spread generated should be reduced. The degree in which tissue spread decreases and potential influences of this method on the human–machine interaction (e.g., the influence of increased pull force) are subjects for future research.

Integrating the teeth into an existing morcellator introduces certain design complexities considering that stacked teeth rings need to be integrated into the morcellation tube (Fig. 3(*b*)). A potentially simple fabrication method is to punch press the teeth into a single piece of sheet metal and bend this sheet metal into a tube shape. To be considered is that the addition of a teeth-bearing tube placed into an existing morcellation tube reduces that instrument's inner diameter. Preferably, the cutting tube should flare open to a larger diameter, allowing for the insertion of a tube with an inner diameter equal to the effective cutting blade diameter. The LiNA Xcise for example has this feature [92].

The presented instrument design (Fig. 11) may be extended to further improve tissue mass control. Going back to both the cookie cutter shark and the lamprey, their use of a suctorial mouth may inspire continued morcellator development. As suggested in several patents [29,32,64], the use of suction to draw tissue into contact with the morcellation instrument, combined with a fluid environment, may be an effective strategy. In light of the recent implementation of laparoscopic containment bags that catch the tissue spread [47,59–61], adding integrated teeth and suction may be a complementary solution to improve morcellation efficacy and safety.

6 Conclusions

Through an iterative design and measurement process, a teeth ring was designed, prototyped, and evaluated with respect to its potential gripping strength on tissue. The evaluation showed that the teeth ring generated grip in the advent of tissue translation and rotation. Stacked teeth rings over a length of 30 mm and having an inner tube diameter of 15 mm provide a theoretical 38 Ncm of torque resistance to prevent the tissue mass from rotating along with the morcellation cutting blade. Future research may implement the proposed design into an already existing morcellator and assess it through an in vitro benchtop evaluation.

Acknowledgment

The authors would like to thank Menno Lageweg and Remi van Starkenburg for their help in fabricating the test facilities and the teeth ring. The research of Ewout A. Arkenbout is supported by the Dutch Technology Foundation STW, which is a part of the Netherlands Organisation for Scientific Research (NWO), and which is partly funded by Ministry of Economic Affairs, Agriculture and Innovation (STW Project 13425).

References

[1] FDA, 2014, "FDA Discourages Use of Laparoscopic Power Morcellation for Removal of Uterus or Uterine Fibroids," Food and Drug Administration, Silver Spring, MD, accessed Apr. 17, 2014, http://www.fda.gov/News Events/Newsroom/PressAnnouncements/ucm393689.htm

[2] Hodgson, B., 2014, "AAGL Practice Report: Morcellation During Uterine Tissue Extraction," J. Minimally Invasive Gynecol., **21**(4), pp. 517–530.

[3] Parker, W. H., Kaunitz, A. M., Pritts, E. A., Olive, D. L., Chalas, E., Clarke-Pearson, D. L., Berek, J. S., and Group, F. T. L. M. R., 2016, "U.S. Food and Drug Administration's Guidance Regarding Morcellation of Leiomyomas: Well-Intentioned, But is It Harmful for Women?," Obstet. Gynecol., **127**(1), pp. 18–22.

[4] Harris, J. A., Swenson, C. W., Uppal, S., Kamdar, N., Mahnert, N., As-Sanie, S., and Morgan, D. M., 2016, "Practice Patterns and Postoperative Complications Before and After U.S. Food and Drug Administration Safety Communication on Power Morcellation," Am. J. Obstet. Gynecol., **214**(1), pp. 98.e91–98.e13.

[5] Desai, V. B., Guo, X. M., and Xu, X., 2015, "Alterations in Surgical Technique After FDA Statement on Power Morcellation," Am. J. Obstet. Gynecol., **212**(5), pp. 685–687.

[6] Brölmann, H., Tanos, V., Grimbizis, G., Ind, T., Philips, K., van den Bosch, T., Sawalhe, S., van den Haak, L., Jansen, F.-W., Pijnenborg, J., Taran, F.-A., Brucker, S., Wattiez, A., Campo, R., O'Donovan, P., and de Wilde, R., 2015, "Options on Fibroid Morcellation: A Literature Review," Gynecol. Surg., **12**(1), pp. 3–15.

[7] Cucinella, G., Granese, R., Calagna, G., Somigliana, E., and Perino, A., 2011, "Parasitic Myomas After Laparoscopic Surgery: An Emerging Complication in the Use of Morcellator? Description of Four Cases," Fertility and Sterility, **96**(2), pp. e90–e96.

[8] Senapati, S., Tu, F. F., and Magrina, J. F., 2015, "Power Morcellators: A Review of Current Practice and Assessment of Risk," Am. J. Obstet. Gynecol., **212**(1), pp. 18–23.

[9] Driessen, S. R. C., Arkenbout, E. A., Thurkow, A. L., and Jansen, F.-W., 2014, "Electromechanical Morcellators in Minimally Invasive Gynecologic Surgery: An Update," J. Minimally Invasive Gynecol., **21**(3), pp. 377–383.

[10] Arkenbout, E. A., van den Haak, L., Driessen, S. R. C., Thurkow, A. L., and Jansen, F.-W., 2015, "Assessing Basic "Physiology" of the Morcellation

Process and Tissue Spread: A Time-Action Analysis," J. Minimally Invasive Gynecol., **22**(2), pp. 255–260.
[11] McCarthy, C., Hussey, M., and Gilchrist, M., 2005, "An Investigation Into the Forces Generated When Cutting Biomaterials With Surgical Scalpel Blades," Key Eng. Mater., pp. 293–294.
[12] McCarthy, C. T., Annaidh, A. N., and Gilchrist, M. D., 2010, "On the Sharpness of Straight Edge Blades in Cutting Soft Solids—Part II: Analysis of Blade Geometry," Eng. Fract. Mech., **77**(3), pp. 437–451.
[13] McCarthy, C. T., Hussey, M., and Gilchrist, M. D., 2007, "On the Sharpness of Straight Edge Blades in Cutting Soft Solids—Part I: Indentation Experiments," Eng. Fract. Mech., **74**(14), pp. 2205–2224.
[14] McGorry, R. W., Dowd, P. C., and Dempsey, P. G., 2003, "Cutting Moments and Grip Forces in Meat Cutting Operations and the Effect of Knife Sharpness," Appl. Ergon., **34**(4), pp. 375–382.
[15] Santhanam, R., and Valenta, H. L., 1996, "Cutting Force Measurements Platform for Quantitative Assessment of Surgical Cutting Instruments," Biomed. Sci. Instrum., **32**(14), pp. 237–243.
[16] Tholey, G., Chanthasopeephan, T., Hu, T., Desai, J. P., and Lau, A., 2003, "Measuring Grasping and Cutting Forces for Reality-Based Haptic Modeling," Int. Congr. Ser., **1256**, pp. 794–800.
[17] Nohilly, M. J., 2008, "Anti-Coring Device for a Surgical Morcellator," U.S. Patent No. 20,080,039,883 (A1).
[18] Nohilly, M. J., Miksza, A. S., and Nering, R., 2010, "Cutting Blade for Morcellator," U.S. Patent No. 2,011,082,485 (A1).
[19] Savage, G. M., Christian, J. J., and Dillow, D. C., 2000, "Disposable Laparoscopic Morcellator," U.S. Patent No. 6039748 (A).
[20] Tutunaru, D., 2006, "Electrical Extractor-Morcellator," U.S. Patent No. RO120451 (B1).
[21] Nohilly, M. J., and Cohn, S., 2012, "Morcellator With Detachable Handle," U.S. Patent No. 2,008,039,884 (A1).
[22] Humphrey, L. E., 1998, "Semi-Automatic Tissue Morcellation Device," U.S. Patent No. 5,746,760 (A).
[23] Poulsen, H. B., 2010, "Surgical Apparatus," U.S. Patent No. 2,012,016,399.
[24] Doll, F., Walter, C., and Roesch, W., 2006, "Surgical Instrument System," U.S. Patent No. 2,006,089,527 (A1).
[25] DuBois, B. R., Nielsen, J. T., and Gordon, A., 2015, "Vacuum Powered Rotary Devices and Methods," U.S. Patent No. 2,015,201,995 (A1).
[26] Wolf, T., 2007, "Morcellator," U. S. Patent No. D535748 (S1).
[27] Sartor, J. D., Westwood, J. G., and Leyva, A. D., 2014, "Devices, Systems, and Methods for Tissue Morcellation," U.S. Patent No. 2,015,018,837 (A1).
[28] Pravong, B., Pravongviengkham, K., Becerra, M. M., Wixey, M. A., Yawata, H., Johnson, G. M., Falkenstein, Z., Brustad, J. R., and Hart, C. C., 2012, "Method and Apparatus for Tissue Morcellation," U.S. Patent No. 2,013,046,140 (A1).
[29] Hooven, M. D., 2000, "Apparatus and Method for Morselating and Removing Tissue From a Patient," U. S. Patent No. WO9624296 (A1).
[30] Jenkins, A. E., Johnston, H. E., and Fleming, A. I., 2014, "Bipolar Surgical Morcellator," U.S. Patent No. 2,015,057,660 (A1).
[31] Ciarrocca, S., 2005, "Bipolar Tissue Morcellator," U.S. Patent No. 2,005,070,892 (A1).
[32] Goble, N. M., 2007, "Electrosurgical Instrument," U.S. Patent No. 7,278,994 (B2).
[33] Goble, N. M., Goble, C. C. O., and Syrop, A. N., 1999, "An Electrosurgical Instrument," U.S. Patent No. WO9903407 (A1).
[34] Hall, M. R., Marshall, M. G., Goble, C. C., Amoah, F., Varney, K. J., and Ebbutt, J. M., 2011, "Surgical Instrument," U.S. Patent No. 2,005,261,676 (A1).
[35] Jenkins, A. E., 2015, "Surgical Instrument," U.S. Patent No. 2,015,250,533 (A1).
[36] Marshall, M. G., Amoah, F., and D'Amelio, F., 2007, "Surgical Instrument," U.S. Patent No. 2,007,219,549 (A1).
[37] Connor, B. G., Sylvester, J. P., Jr., Modoono, P. T., Staid, K. P., and Reed, D. M., 2004, "Surgical Devices Incorporating Liquid Jet Assisted Tissue Manipulation and Methods for Their Use," U.S. Patent No. 2,004,243,157 (A1).
[38] Hart, S. R., Esinhart, E. J., Lytle, A. T., Kamsler, D. R., Drake, C. W., III, Junaideen, Y. A., and Simoes, M. A., 2015, "Minimally Invasive Laparoscopic Tissue Removal Device," U. S. Patent No. 20,150,335,342.
[39] Pfeffer, H. G., and Wilk, P. J., 1998, "Method and Apparatus for Organic Specimen Retrieval," U.S. Patent No. 5,735,289 (A).
[40] Tah, R. C., Ciulla, R., and Weiser, M. F., 2014, "Retrieval Device and Related Methods of Use," U.S. Patent No. 2,014,276,913 (A1).
[41] Isakov, A., Murdaugh, K., Burke, W., Einarsson, J. I., and Walsh, C., 2014, "System and Method for a Laparoscopic Morcellator," U.S. Patent No. WO2014158880 (A1).
[42] van den Haak, L., Arkenbout, E. A., Sandberg, E. M., and Jansen, F. W., 2016, "Power Morcellator Features Affecting Tissue Spill in Gynecologic Laparoscopy: An In-Vitro Study," J. Minimally Invasive Gynecol., **23**(1), pp. 107–112.
[43] Protsenko, D. E., and Pearce, J. A., 2003, "Electrosurgical Tissue Resection: A Numerical and Experimental Study," Proc. SPIE, **4954**, pp. 64–70.
[44] Milad, M. P., and Milad, E. A., 2014, "Laparoscopic Morcellator-Related Complications," J. Minimally Invasive Gynecol., **21**(3), pp. 486–491.
[45] de Boorder, T., Verdaasdonk, R., and Klaessens, J., 2007, "The Visualization of Surgical Smoke Produced by Energy Delivery Devices: Significance and Effectiveness of Evacuation Systems," Proc. SPIE, **6440**, p. 64400.
[46] Varkarakis, J. M., McAllister, M., Ong, A. M., Solomon, S. B., Allaf, M. E., Inagaki, T., Bhayani, S. B., Trock, B., and Jarrett, T. W., 2004, "Evaluation of Water Jet Morcellation as an Alternative to Hand Morcellation of Renal Tissue Ablation During Laparoscopic Nephrectomy: An In Vitro Study," Urology, **63**(4), pp. 796–799.
[47] Rimbach, S., Holzknecht, A., Schmedler, C., Nemes, C., and Offner, F., 2016, "First Clinical Experiences Using a New In-Bag Morcellation System During Laparoscopic Hysterectomy," Arch. Gynecol. Obstet., **294**(83), pp. 1–11.
[48] Rassweiler, J., Stock, C., Frede, T., Seemann, O., and Alken, P., 1998, "Organ Retrieval Systems for Endoscopic Nephrectomy: A Comparative Study," J. Endourology, **12**(4), pp. 325–333.
[49] Lehmann, A. L., Radl, C. L., Smith, T., and Vennel, M. R., 2015, "Entrapment and Containment System for Use With a Morcellator and Method of Entrapping and Containing Material Produced During Morcellation Procedure," U.S. Patent No. 2,015,320,409.
[50] Collins, J., 2011, "Medical Device: Laparoscopic Bag," U.S. Patent No. 2,014,135,788 (A1).
[51] Shibley, K. A., Bonadio, F., Vaugh, T., and MacNally, S. J., 2012, "Pneumoperitoneum Device," U.S. Patent No. 2,013,184,536 (A1).
[52] Hoyte, L., and Imudia, A., 2015, "Power Morcellation in a Protected Environment," U.S. Patent No. CA2,888,700 (A1).
[53] Jospeh, L., 2015, "Safety Isolation Bags for Intra Abdominal, Endoscopic Procedures, Power Morcellation and Vaginal Morcellation," U.S. Patent No. IN4189CH2015(A).
[54] Clayman, R. V., and Pingleton, E. D., 1992, "Surgical Containment Apparatus," U.S. Patent No. EP0,465,051 (A2).
[55] Wachli, S., Breslin, T., Kessler, S., Poulsen, N., Collins, N., Do, A., Bolanos, E., Pravong, B., Elliott, P., Wixey, M., Young, W., Filek, J., Castelo, K., Hoke, A., Hofstetter, G., Demarchi, J., Garces, A., Holmes, H., and Sheehan, A., 2015, "Systems and Methods for Tissue Removal," U.S. Patent No. WO2,015,164,591 (A1).
[56] Kondrup, J. D., Sylvester, B. A., and Branning, M. L., 2015, "Tissue Debris and Blood Collection Device and Methods of Use Thereof," U.S. Patent No. 2015272561 (A1).
[57] Spaeth, E. E., Borsanyi, A. S., Bowie, A., and Sorensen, J. T., 1993, "Trocar System for Facilitating Passage of Instruments Into a Body Cavity Through a Minimal Access Incision," U.S. Patent No. 5,224,930 (A).
[58] Hart, S. R., Hipol, P. J., Simoes, M. A., and Zakaria, M. A., 2014, "Transvaginal Specimen Extraction Device," U.S. Patent No. 2,014,288,486 (A1).
[59] Cohen, S. L., Greenberg, J. A., Wang, K. C., Srouji, S. S., Gargiulo, A. R., Pozner, C. N., Hoover, N., and Einarsson, J. I., 2014, "Risk of Leakage and Tissue Dissemination With Various Contained Tissue Extraction (CTE) Techniques: An In Vitro Pilot Study," J. Minimally Invasive Gynecol., **21**(5), pp. 935–939.
[60] Einarsson, J. I., Cohen, S. L., Fuchs, N., and Wang, K. C., 2014, "In-Bag Morcellation," J. Minimally Invasive Gynecol., **21**(5), pp. 951–953.
[61] Paul, P. G., Thomas, M., Das, T., Patil, S., and Garg, R., 2015, "Contained Morcellation for Laparoscopic Myomectomy Within a Specially Designed Bag," J. Minimally Invasive Gynecol., **23**(2), pp. 257–260.
[62] Mohamed, Z., and McDonald, T. D., 2012, "Medical Device and Method for Human Tissue and Foreign Body Extraction," U.S. Patent No. 2,009,326,546 (A1).
[63] Li, L. K., 1995, "Morcellator System," U.S. Patent No. 5,443,472 (A).
[64] Sorensen, J. T., Limonta, F., and Dial, L. A., 1997, "Tissue Morcellator System and Method," U.S. Patent No. 5,618,296 (A).
[65] Vaitekunas, J. J., 2000, "Method of Tissue Morcellation Using an Ultrasonic Surgical Instrument With a Ballistic Specimen Bag," U.S. Patent No. 6,162,235 (A).
[66] Fox, W. D., and Parkhurst, H. C., 1996, "Mechanical Morcellator," U.S. Patent No. 5,520,634 (A).
[67] Saad, A. H., 2014, "Surgical Device Having an Inner Thread and a Sharpening Device for Such a Device," U.S. Patent No. 20,140,276,912.
[68] Sartor, J. D., and Heard, D. N., 2014, "System for Myomectomy and Morcellation," U.S. Patent No. 2,015,073,224 (A1).
[69] Sauer, J. S., Greenwald, R. J., Bovard, M. A., and Hammond, J. F., 1996, "Morcellator," U.S. Patent No. 5,562,694 (A).
[70] Shadduck, J. H., Germain, A., Truckai, C., Walker, M. D., and Klein, K., 2012, "Laparscopic Tissue Morcellator Systems and Methods," U.S. Patent No. 2,013,090,642 (A1).
[71] Cohen, S. L., Morris, S. N., Brown, D. N., Greenberg, J. A., Walsh, B. W., Gargiulo, A. R., Isaacson, K. B., Wright, K. N., Srouji, S. S., Anchan, R. M., Vogell, A. B., and Einarsson, J. I., 2016, "Contained Tissue Extraction Using Power Morcellation: Prospective Evaluation of Leakage Parameters," Am. J. Obstet. Gynecol., **214**(2), pp. 257.e251–257.e256.
[72] Solima, E., Scagnelli, G., Austoni, V., Natale, A., Bertulessi, C., Busacca, M., and Vignali, M., 2015, "Vaginal Uterine Morcellation Within a Specimen Containment System: A Study of Bag Integrity," J. Minimally Invasive Gynecol., **22**(7), pp. 1244–1246.
[73] Urban, D. A., Kerbl, K., McDougall, E. M., Stone, A. M., Fadden, P. T., and Clayman, R. V., 1993, "Organ Entrapment and Renal Morcellation: Permeability Studies," J. Urol., **150**(6), pp. 1792–1794.
[74] Ankem, M. K., Hedican, S. P., Pareek, G., Waterman, B. J., Moon, T. D., Selvaggi, S. M., and Nakada, S. Y., 2006, "Examination of Laparoscopic Retrieval Bag Washings for Malignant Cells After Hand-Assisted Laparoscopic Radical Nephrectomy and Intact Specimen Removal," Urology, **68**(1), pp. 50–52.
[75] Fentie, D. D., Barrett, P. H., and Taranger, L. A., 2000, "Metastatic Renal Cell Cancer After Laparoscopic Radical Nephrectomy: Long-Term Follow-Up," J. Endourology, **14**(5), pp. 407–411.
[76] Johnston, N. E., 2014, "The Avian Tongue," Golden Gate Audubon Society, San Francisco, CA, accessed Oct. 15, 2016, http://goldengateaudubon.org/wp-content/uploads/Avian-Tongues_Johnston.pdf
[77] Spotila, J. R., 2004, *Sea Turtles: A Complete Guide to Their Biology, Behavior, and Conservation*, JHU Press, Baltimore, MD.

[78] Lutz, P. L., and Musick, J. A., 1997, *The Biology of Sea Turtles*, CRC Press, Boca Raton, FL.
[79] Whitenack, L. B., 2008, "The Biomechanics and Evolution of Shark Teeth," Ph.D. thesis, University of South Florida, Tampa, FL.
[80] Bels, V. L., Aerts, P., Chardon, M., Vandewalle, P., Berkhoudt, H., Crompton, A., de Vree, F., Dullemeijer, P., Ewert, J., and Frazzetta, T., 2012, *Biomechanics of Feeding in Vertebrates*, Springer Science & Business Media, Berlin.
[81] Richard, W., 2016, "Morce Power Plus, Effective and Ergonomic Morcellation," Richard Wolf GmbH, Knittlingen, Germany, accessed June 13, 2016, http://www.richard-wolf.com/broschueren/Gynecology/E_632_MorcePower_plus_VIII14_EN.pdf
[82] Arkenbout, E. A., 2012, "Design Process of a Trans-Vaginal Morcellator for Total Laparoscopic Hysterectomy; From Clinical Functionality Assessment to First Prototype," Master thesis, TU Delft, Delft University of Technology, Delft, The Netherlands.
[83] Nouvag, 2016, "TCM 3000 BL—Morcellator for Laparoscopic Hysterectomy," NOUVAG AG, Goldag, Switzerland, accessed Feb. 8, 2016, http://www.nouvag.com/en/medical/laparoscopic-hysterectomy/morcellator-system/559-tcm-3000-bl-morcellator.html
[84] Axtrocare, 2016, "Morcellator Moresolution," Axtrocare, Donaueschingen, Germany, Oct. 15, 2016, http://www.axtrocare.com/cms/fileadmin/user_upload/produkte/morcellator/Image-Morcellator_EN. pdf.
[85] van Gerwen, D. J., Dankelman, J., and van den Dobbelsteen, J. J., 2012, "Needle–Tissue Interaction Forces—A Survey of Experimental Data," Med. Eng. Phys., **34**(6), pp. 665–680.
[86] Heijnsdijk, E. A. M., Dankelman, J., and Gouma, D. J., 2002, "Effectiveness of Grasping and Duration of Clamping Using Laparoscopic Graspers," Surg. Endoscopy Interventional Tech., **16**(9), pp. 1329–1331.
[87] Cheng, L., and Hannaford, B., 2016, "Evaluation of Liver Tissue Damage and Grasp Stability Using Finite Element Analysis," Comput. Methods Biomech. Biomed. Eng., **19**(1), pp. 31–40.
[88] Marucci, D. D., Cartmill, J. A., Walsh, W. R., and Martin, C. J., 2000, "Patterns of Failure at the Instrument–Tissue Interface," J. Surg. Res., **93**(1), pp. 16–20.
[89] Brown, A. W., Brown, S. I., McLean, D., Wang, Z., and Cuschieri, A., 2014, "Impact of Fenestrations and Surface Profiling on the Holding of Tissue by Parallel Occlusion Laparoscopic Graspers," Surg Endoscopy Interventional Tech., **28**(4), pp. 1277–1283.
[90] Heijnsdijk, E. A. M., Visser, H., Dankelman, J., and Gouma, D. J., 2004, "Slip and Damage Properties of Jaws of Laparoscopic Graspers," Surg. Endoscopy Interventional Tech., **18**(6), pp. 974–979.
[91] Heijnsdijk, E. A. M., Kragten, G. A., Mugge, W., Dankelman, J., and Gouma, D. J., 2005, "Fenestrations in the Jaws of Laparoscopic Graspers," Minimally Invasive Ther. Allied Technol., **14**(1), pp. 45–48.
[92] LiNA Medical, 2016, "LiNA Xcise Cordless Laparoscopic Morcellator," LiNA Medical, Glostrup, Denmark, accessed Oct. 15, 2016, http://www.lina-medical.com/products/lina-xcise/
[93] Gilkeson, J., 2015, "Duluth Boat Show—Sea Lamprey Booth," U.S. Fish and Wildlife Service, Washington, DC.